

## QUANTIFICATION OF IMAGE DATA AND A KINETIC MODEL FOR THE INTEGRIN RECEPTOR MOVEMENT ON THE SURFACE OF LIVING CELLS

IVAYLO ZLATANOV, THOMAS GROTH<sup>†</sup> and GEORGE ALTANKOV

*Institute of Biophysics, Bulgarian Academy of Sciences  
Acad. G. Bonchev Str., Bl. 21, 1113 Sofia, Bulgaria*

<sup>†</sup>*GKSS Research Center, Institute of Chemistry  
Kantstrasse 55, D-14513 Teltow, Germany*

**Abstract.** Living human fibroblasts were attached on fibronectin coated surfaces and stained with FITC labeled anti- $\beta_1$  integrin monoclonal antibody. The dynamic behaviour of these integrin–antibody complexes were then observed within 2.5 hours by periodic scans using confocal laser scanning microscope. Obtained data were used for analyzing the initial  $\beta_1$  integrin reorganizations during fibroblasts spreading on fibronectin. Pursuing this aim, a specific physical model and mathematical algorithm was created that permit the corrections of the noise and the fluorescence photobleaching during the scanning. Using specific image analyzing software were defined three “regions of interest” (ROI) and the kinetic changes of integrin densities, as well as, the individual velocity of receptor clusters movement were quantified. Calculated velocities provide novel quantitative information about the centripetal movement of  $\beta_1$  integrins on the dorsal cell surface of fibroblasts upon ligand binding.

### 1. Introduction

Integrins are cell surface receptors, which play an important role for the communication of the cells with their **extracellular matrix** (ECM) [12, 30, 10]. As transmembrane heterodimers they bind to the specific adhesive proteins and link them to the cytoskeleton [7, 11, 16, 33, 35], thus accomplishing a specific “mechanical” crosstalk [10] between the cell and the surrounding adhesive matrix.

In the process of cell-to-ECM interactions the mobility of the integrins play an important role and currently they are a topic of an extensive scientific interest [10, 23, 32, 35].

There are different attempts to measure the speed of the integrins utilizing diverse experimental approaches. The method of **fluorescence recovery after photobleaching** (FRAP) had been applied by Duband *et al* [9] and register lateral diffusion coefficients in the range of  $2 \times 10^{-10}$  to  $4 \times 10^{-10}$  cm<sup>2</sup>/s, which is equal to velocities of 0.283 to 0.4  $\mu$ m/min of integrin clusters in avian embryonic cells. Using similar technique Palecek *et al* [21] measured speeds from 0.0167 to 1.333  $\mu$ m/min in chicken skeletal myofibroblasts. Kawakami *et al* [14] applied the method of time-lapse total-internal-reflection fluorescence microscopy and reported  $0.29 \pm 0.24$   $\mu$ m/min for vein endothelial cells. All these methods however are appropriate for chaotically moved particles.

In living cell the centripetal flow of cytoplasm result in movement of integrins from the periphery to the cell center. Smilenov *et al* [25] demonstrated that the focal contacts, the adhesive clusters of integrins on the **ventral cell surface**, can also move centripetally in living non-motile fibroblasts with average speed of  $0.12 \pm 0.08$   $\mu$ m/min. Katz *et al* [13] further show that the focal contacts are able to grow, fade or translocate centripetally. These so called fibrillar adhesions however, segregate from the peripheral focal contacts and move to the cell center. Pankov *et al* [22] reported that antibody-bound  $\alpha_5\beta_1$  integrins can actively translocate along the small actin-filament bundles [10] with average speed of  $0.108 \pm 0.012$   $\mu$ m/h. These studies however, concern the movement of integrins on the ventral cell surface (faced to the substratum) while very little is known about the behavior of integrins on the dorsal cell surface. The later contains a larger part of integrins, but their function is not very clear. It was a main goal of the present study to visualize these dorsal integrins in living cells via binding with fluorescently labeled antibodies and to study their dynamic behaviour upon antibody-tag. Following these aim we used a confocal laser scanning fluorescence microscopy to visualize integrin clusters in living cells. In fact, by periodical scans we created image series, which were organized as movies. However, binding of monoclonal antibodies mimic to a certain extent the physiological ligand occupation [18, 19] and triggers directly [3, 6, 8, 15, 20] the  $\beta_1$  integrin clustering and movement. Thus, we got a system for studying the behavior of activated integrins located predominantly at the dorsal cell surface.

To quantify and analyze integrin dynamics we further develop a kinetic model and special algorithm for calculation of dynamical changes of integrin densities at different cell zones and these kinetic expressions finally allowed us to calculate the speed and to characterize the dynamic behaviour of above activated integrins.

## 2. Materials and Methods

### 2.1. Cells

Human fibroblasts were obtained from fresh skin biopsies and used up to the tenth passage. Cells were grown in Dulbeccos modified Eagle's medium (DMEM) containing 10% **fetal calf serum** (FCS) (Sigma Chemicals Co., St. Louis, MO) in a humidified incubator with 5% CO<sub>2</sub>. Fibroblasts from pre-confluent cultures were harvested with 0.05% trypsin/0.6 mM EDTA (Sigma). Trypsin was neutralized with FCS. Then cells were placed in self-constructed microscopic cell culture chamber. Briefly, standard silicon spacer (FlexiPerm, Town, Germany) were attached onto round shaped microscopic glass slides with diameter of 35 mm (PeCon GmbH, Erbach-Buch, Germany) previously cleaned with ethanol and phosphate buffered saline (PBS) containing 150 mM NaCl, 5.8 mM Na<sub>2</sub>HPO<sub>4</sub> and 5.8 mM NaH<sub>2</sub>PO<sub>4</sub>. The resulting surfaces at the bottom of chambers were coated with 20 µg/ml **fibronectin** (FN) in PBS at room temperature for 30 min, and subsequently washed with PBS and DMEM. Approximately  $5 \times 10^3$  fibroblasts in 450 µl serum free DMEM were added to each chamber and incubated for 1 h in a humidified CO<sub>2</sub> incubator at 37 °C to give time for appropriate cell attachment and spreading.

### 2.2. Fluorescent Antibody Staining of Integrins and Fluorescent Standards

Flasks with cells were removed from the incubator, cooled to 4 °C and then incubated for 10 min with a FITC-conjugated anti  $\beta_1$  integrin monoclonal antibody (CD29, Biosource, Int., USA, Cat. No. 2908) diluted 1:50 in 100 µl DMEM containing 10% FN-free FCS. Before hand the FN was removed from the serum by gelatin-Sepharose 4B (Pharmacia, Sweden). Then, the cells were washed three times with DMEM to remove the non-bound antibody and finally immersed in 450 µl DMEM, containing 10% FN-free FCS.

Fluorescent standards were prepared by dissolving of 10 µl of the same fluorescent antibody in 200 µl worm (40°C) Moviol (Kuraray Specialities Europe, GmbH, Germany) and mixed carefully. A drop of this mixture was then sliced on a round 35 mm microscope glass and dried for 24 hours at room temperature. So prepared standards were scanned many times under CLSM just at the same conditions and laser intensities as the cells.

### 2.3. Confocal Laser Scanning Microscopy (CLSM)

Time lapse microscopy was performed with a confocal laser scanning microscope type LSM 510 (Carl Zeiss, Jena, Germany) equipped with thermostatic chamber type "Temp-control 37-2", (PeCon GmbH, Jena, Germany). The latter was fitted

to the microscope stage. Glass slides together with the attached silicon chamber were placed inside. The temperature at the bottom of the sample was precisely adjusted to 37°C by a calibrated thermocouple. Single cells were scanned every 10 min using the automated time-lapse series mode up to 2.5 h.

As described previously [37] image sequences were exported by LSM Image Examiner software in TIFF format and captured on the hard drive in separate folders. Due to cellular movements some images were out of focus and were discarded.

#### 2.4. Image Analysis

The remaining images in the time sequences were processed and analyzed by the freely available java-based public domain software **ImageJ**, version 1.32a, developed at the National Institutes of Health (NIH), Bethesda, MD (<http://rsb.info.nih.gov/ij/>). Using the “Region of Interest Manager” and the tool “Freehand Selection” of this program, it was possible to specify different regions of the investigated cell and then quantify the fluorescence (mean gray value), area and their standard deviations in this chosen selection.

To analyze the behavior of integrins we measured the individual velocities of the integrins. Watching the movies one can easily recognize single integrin-antibody clusters moving centripetally. We choose an appropriate cluster and measured its velocity estimating the coordinates on few consecutive images in the time-lapsed series. Briefly, using the “mark and count” tool of the ImageJ we marked the moving particle in one of the time-lapsed pictures and thus obtained the coordinates  $x_1, y_1$  at time  $t_1$ . Watching the next picture of the sequence we marked the same cluster and counted its new coordinates  $x_2, y_2$  at time  $t_2$ . Knowing these coordinates one can calculate the distance between point  $x_1, y_1$  and  $x_2, y_2$  in pixels and further convert the distances in  $\mu\text{m}$ . Times  $t_1$  and  $t_2$  we also know exactly from the data of the image sequence (using CLSM tools “Gallery” and “Data”). We measured a sufficient number of clusters (at least 10) in different cell regions.

#### 2.5. Physical Model and Mathematical Algorithm

In respect to analyze the mass redistribution and centripetal flow of integrin receptors we create a model for quantification of the image parameters based on the following:

Part of the fluorescent antibodies bind to  $\beta_1$  integrins during the labeling procedure. Since non-bound antibodies were removed by washing, we accept that the quantity of bound antibody remains constant during the experiment and is proportional to the number  $N$  of labeled receptors. Hence, the fluorescence  $F$  of the whole cell is

$$F = \text{const} \times N. \quad (1)$$

The specific fluorescence  $F_{sp}$  is defined as fluorescence of a single area  $A$

$$F_{sp} = F/A = \text{const} \times (N/A). \quad (2)$$

The ratio  $N/A$  however represents the density of integrin receptors for the selected region of the cell, and thus equation (2) gives a direct expression of density by the fluorescence. Both parameters  $F$  and  $A$  were measured by the plug-in “Analyze” of ImageJ.

We defined three zones of special region of interest (SROI) that are well recognized in most of the cells (see Fig. 1) namely: a **peripheral zone** (PZ) respectively SROI<sub>1</sub>, a **middle zone** (MZ), SROI<sub>2</sub> and a central or **nuclear zone** (NZ) SROI<sub>3</sub>. The ROI's at time  $t_1$  (i.e. the first image of a given cell in the time series) were created by “Freehand selection” of ImageJ as shown in Fig. 1. ROI<sub>1</sub> includes the whole cell area (marking the contour of the cell), ROI<sub>2</sub> includes both the middle

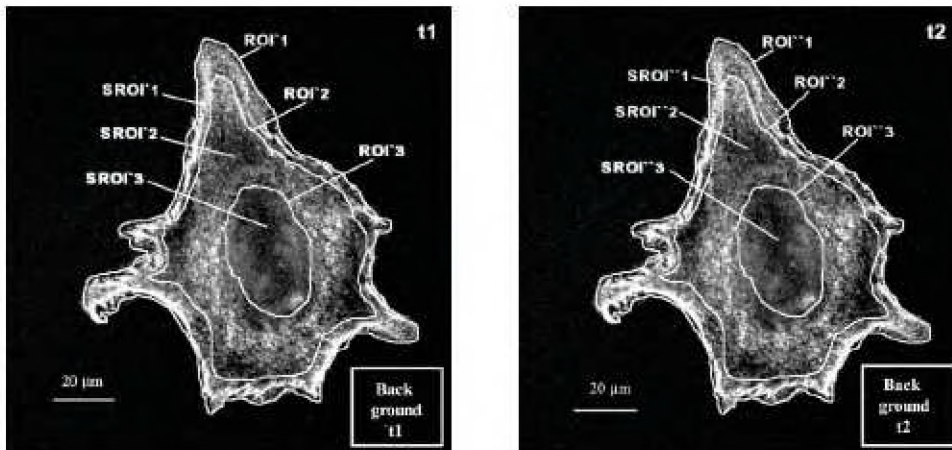


**Figure 1.** Example for construction of regions of interest (ROI) on images of fibroblast, made at two different moments  $t_1$  and  $t_2$ . First ROI<sub>1</sub> includes all of the cell area. Second ROI<sub>2</sub> includes the middle and central (nuclear) zone and third ROI<sub>3</sub> includes only the central zone. Areas  $A_{t_n}$  and fluorescence  $F_{t_n}$  of these areas are measured at different moments  $t_n$ . First special region of interest (SROI<sub>1</sub>) is the strip between ROI<sub>1</sub> and ROI<sub>2</sub>. This strip covers the periphery of the cells, where the most of focal contacts are located. Second strip between ROI<sub>2</sub> and ROI<sub>3</sub> covers SROI<sub>2</sub> of the middle zone and SROI<sub>3</sub> coincides with the central nuclear zone. Rectangles covered a part of the background outside of the cell have areas  $A_b^{t_1}$ ,  $A_b^{t_2}$  and fluorescence  $F_b^{t_1}$ ,  $F_b^{t_2}$ , respectively. ROI's were drawn by hand, fluorescence intensities and areas were measured by using image analyzing ImageJ software (<http://rsb.info.nih.gov/ij/>).

and the nuclear zone, and ROI<sub>3</sub> includes the nuclear zone only. At each time  $t_n$  in the time series the ROI's were defined by the same way and named ROI<sub>1</sub> <sup>$t_n$</sup> , ROI<sub>2</sub> <sup>$t_n$</sup>  and ROI<sub>3</sub> <sup>$t_n$</sup> , respectively. The parameters that we measured were the fluorescence  $F_m^{t_n}$  ( $m = 1, 2, 3, \dots$  is the number of ROI;  $n = 1, 2, 3, \dots$  is the number of analyzed images in a time-lapsed series) and the respective area of the cell is  $A_m^{t_n}$ . Thus, measuring the changes in these parameters with time, we have investigated the dynamics of integrin receptor redistribution.

The specific fluorescence of the peripheral zone is

$$F_{\text{pzs}}^{\text{sp}} = (F_1^{t_n} - F_2^{t_n}) / (A_1^{t_n} - A_2^{t_n}). \quad (3)$$

To eliminate background fluorescence and other noises of the system, at every time  $t_n$  we measured the fluorescence  $F_b^{t_n}$  and the area  $A_b^{t_n}$  of a defined segment from the background outside the cell (see the marked squares in Fig. 1). Thus, the specific fluorescence of the background is

$$F_b^{\text{sp}} = F_b^{t_n} / A_b^{t_n} \quad (4)$$

and studying the ratio  $F_{\text{pzs}}^{\text{sp}} / F_b^{\text{sp}}$  from equations (3) and (4) we obtain a non-dimensional signal-to-noise ratio  $D_{\text{pzs}}^{t_n}$ , which is a function of  $t_n$  and proportional to the real density of the receptors:

$$D_{\text{pzs}}^{t_n} = \text{const} \times [(F_1^{t_n} - F_2^{t_n}) \times A_b^{t_n}] / [F_b^{t_n} \times (A_1^{t_n} - A_2^{t_n})]. \quad (5)$$

The relation of this density to the initial one at time  $t_1$  is

$$\frac{D_{\text{pzs}}^{t_n}}{D_{\text{pzs}}^{t_1}} = \frac{[(F_1^{t_n} - F_2^{t_n}) \times A_b^{t_n}] \times [F_b^{t_1} \times (A_1^{t_1} - A_2^{t_1})]}{[(F_1^{t_1} - F_2^{t_1}) \times A_b^{t_1}] \times [F_b^{t_n} \times (A_1^{t_n} - A_2^{t_n})]}. \quad (6)$$

For example, when the density in the peripheral zone  $D_{\text{pzs}}$  changes with the time, as a result of receptor movement,  $D_{\text{pzs}}$  becomes also a function of the time.

If we assume that the initial density is 100% = 1, then from equation (6) we obtain

$$D_{\text{pzs}}^{t_n} = \frac{[(F_1^{t_n} - F_2^{t_n}) \times A_b^{t_n}] \times [F_b^{t_1} \times (A_1^{t_1} - A_2^{t_1})]}{[(F_1^{t_1} - F_2^{t_1}) \times A_b^{t_1}] \times [F_b^{t_n} \times (A_1^{t_n} - A_2^{t_n})]}. \quad (7)$$

Because all parameters in the right side of this expression are measurable, we are able to plot the obtained kinetics of integrin density in PZ as a relative change to the initial density. The densities for the middle and nuclear zones were obtained following the same procedure

## 2.6. Corrections for Photo-Bleaching

As we assumed above, the quantity of receptors in the whole cell remains constant during the experiment and the bleaching affects only the fluorescence intensity as

a function of the number of scans. Using the specific fluorescence of the first ROI<sub>1</sub> as a base we can define a correction function as follows

$$K(p) = [F_1^1/A_1^1]/[F_1^p/A_1^p]. \quad (8)$$

$F_1^1$  and  $A_1^1$  are the fluorescence and the area of the whole cell (ROI<sub>1</sub>) at the first scan.  $F_1^p$  and  $A_1^p$  are the fluorescence and area at scan  $p$ . Note, the number of scans  $p$  was sometimes different from the number of individual images  $m$  because we discarded images that were not focused due to cellular movements. From the experimental protocols however, we know how many scans were made, as well as, the respective time  $t_n$ . Hence, we can substitute the argument  $p$  by time  $t_n$  in equation (8) to obtain the correction function

$$K(t_n) = [F_1^1/A_1^1]/[F_1^{t_n}/A_1^{t_n}]. \quad (9)$$

Then, the correction for bleaching in the peripheral zone (equation (9)) is

$${}^{\text{corr}}D_{\text{pz}}^{t_n} = K^{t_n} \times D_{\text{pz}}^{t_n}. \quad (10)$$

This correction function is specific for each single cell and was used for the peripheral, middle and nuclear zones of the same cell. Finally, the data for fluorescence and areas of the different regions were processed with the Origin software (<http://www.originlab.com/>). Calculations according to equation (10) were performed to plot kinetics and to fit the experimental curves with different models (exponential or linear functions).

### 3. Results

#### 3.1. Speed of the Integrin Receptors

Integrin clusters in PZ and MZ move centripetally from the periphery to the center of the cell. Speeds of 48 well visible integrin clusters in PZ of four different cells were measured directly. The mean speed was calculated at level of significance  $p < 0.05$  as  $0.353 \pm 0.02 \mu\text{m}/\text{min}$ , where 0.02 is the **standard error** (SE) of the mean. Respectively 44 integrin clusters were measured in the MZ of four cells and calculated mean speed was  $0.52 \pm 0.03 \mu\text{m}/\text{min}$  ( $p < 0.05$ ).

In the central NZ centripetal movement was absent but we have measured the mean speed of 44 chaotically moving integrin clusters, in the same four cells. It was  $0.435 \pm 0.04 \mu\text{m}/\text{min}$  ( $p < 0.05$ ).

At a level of significance  $p < 0.05$  the speed in MZ was the highest, followed by the speed in NZ, and finally the speed in PZ was the lowest.

### 3.2. Measurements of the Bleaching Effect and Correction Function

This effect was measured by using the above described fluorescent standards, scanned at the same conditions (488 nm laser beam) as the living cells. Following equation (4), the specific fluorescence as a function of scan number was measured and the results are presented in Fig. 2. The experimentally obtained data (Panel A

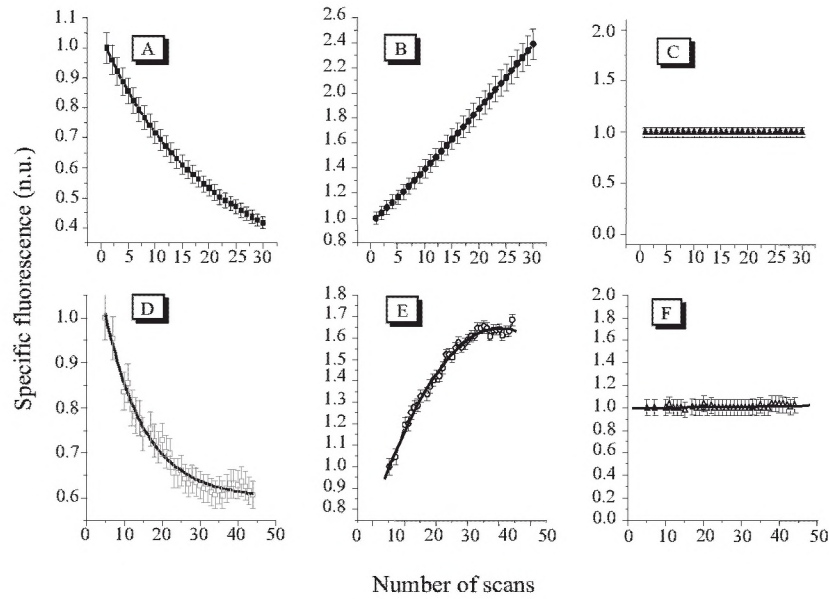


**Figure 2.** Correction of bleaching effect. Results of measuring the specific fluorescence (intensity/area) of standard as described in Section 2, are shown in Panel A. The specific fluorescence  $Q$  of all the area ( $ROI_1$ ) of a single cell are presented in Panel D. Panels B and E represent the respective correction coefficients (functions) calculated by expression (9). Finally, the corrected specific fluorescence is shown on Panels C and F. Each point represents the mean values of three independent measurements and the vertical bars show the standard error.

and D) fit better to an exponential decay of first order

$$F_{sp}(n) = F_{min} + \nu \cdot e^{-n/s} \quad (11)$$

where  $n$  is the number of scans,  $\nu$  and  $s$  are coefficients and  $F_{min}$  is the fluorescence at  $n \rightarrow \infty$ . In Table 1 we present the values of the fit parameters demonstrating an exponential decay of fluorescence at 488 nm of illumination, independently of where FITC-conjugated antibody is incorporated, in the artificial medium (Moviol) of the standard, or in the surface membrane of the living cell.

**Table 1**

Parameter	$\nu$	$s$	$F_{\min}$ (at $n \rightarrow \infty$ )
Fl. standard	$0.777 \pm 0.047$	$19.2 \pm 3.5$	$0.257 \pm 0.063$
Living cell	$0.736 \pm 0.053$	$10.5 \pm 0.66$	$0.599 \pm 0.0065$

As far as experimental data in Fig. 2 are normalized, these results mean that after many scans only 25.7% of the initial fluorescence remains in the standard probes and about 60 % in the living cell.

One can see however, that corrected fluorescence intensities in Panels C and F of Fig. 2 are close to horizontal straight lines, demonstrating that suggested algorithm for corrections of the bleaching and noise effects is usable for the calculations below.

The correction coefficients in Panel E are specific for a given cell and were used for correction of the bleaching effect in calculations for all regions (ROI's) of this cell. Analysis of another cell needs new measurements and new calculations of its specific correction function.

Apparently the bleaching effect on FITC in the cell is significantly lower as a result of the FRAP because conditions for movement of the fluorescent clusters in the membrane of the living cell are better. Presumably some non-destroyed FITC-labeled molecules can arrive from the regions, which are out of focus during the microscopy. Vice versa, in the fluorescent standards fluorescent antibodies are less movable and the renovation with unbleached molecules is almost impossible.

### 3.3. Quantification of the Integrin Dynamics and Redistribution of the Receptors

It was well visible in time-lapsed series (available also as a video clip in the web at [http://www.bio21.bas.bg/ibf/dpb\\_files/iz/Supplement1.avi](http://www.bio21.bas.bg/ibf/dpb_files/iz/Supplement1.avi)) that integrin particles move and re-distribute after the addition of antibody. To obtain an analytical view on this process, we measured the fluorescence intensities along a line segment from the periphery to the center of the cell (Panel A in Fig. 3), using the instrument "Plot Profile" of the software ImageJ. Thus, images (scans) of the cell, made at the 30th, 60th, 90th and 120th minute after the fluorescent labeling were analyzed and the results are present in Panels B, C, D and E of Fig. 3. Experimental points represent mean values of ten measurements, made by moving transversely the line segment in the chosen region of the cell (Panel A) by step of 0.1  $\mu\text{m}$ .

Time-dependent changes in the form of fluorescence profiles are well defined, demonstrating the redistribution of integrins. A decrease of the fluorescence in PZ and the cell center were found. Significant changes are also visible in the middle

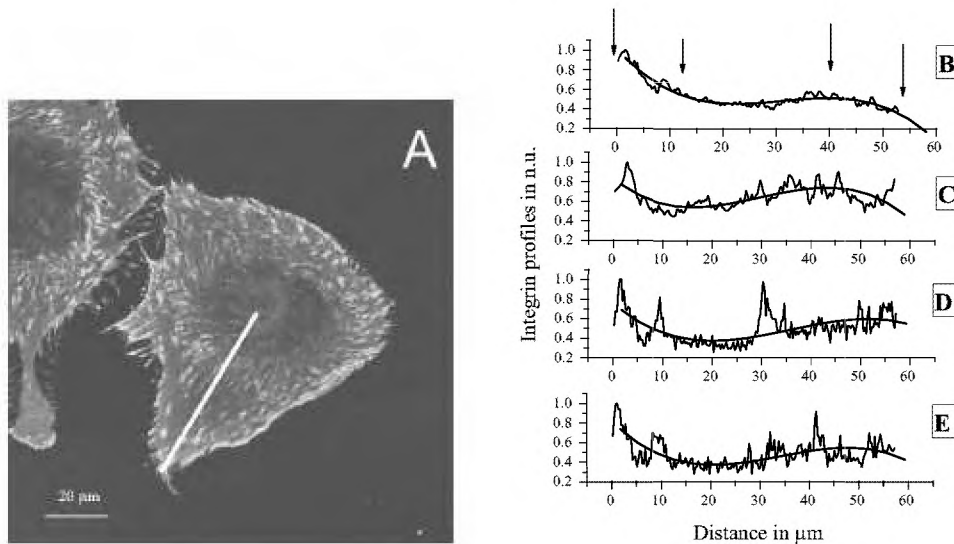


**Figure 3.** Profiles of integrin quantity along the line segment (Panel A) drawn from the periphery to the cell center. Measurements were made by the plug-in “Plot Profile” of the image-analyses software “ImageJ” (<http://rsb.info.nih.gov/ij/>). Experimental points represent the mean values of ten measurements of the fluorescence intensities captured by step of  $0.1\ \mu\text{m}$ . Fit curves were made as polynomial model of 4th degree. The measurements were performed on individual images of a living cell captured on the 30th (panel B), 60th (Panel C), 90th (Panel D) and 120th (Panel E) minutes after labeling of the integrin receptors with fluorescent antibody. Vertical arrows in Panel B indicate the approximate borders of the different zones, as follows: the width of the PZ is  $0\text{--}12\ \mu\text{m}$ ; the MZ is  $12\text{--}35\ \mu\text{m}$ , and the NZ is  $35\text{--}53\ \mu\text{m}$ .

and nuclear zones. These profiles however, could be rather a basis for qualitative analysis and represents our first attempt to quantify the dynamics of integrin redistribution

To better analyze the dynamical behaviour of integrins we applied the algorithm, described in Section 2. Four time-lapsed movies of cells from different experiments were quantified, and Fig. 4 shows a typical result. The initial quantity of integrins (during the first scan) was distributed as follows:  $Q_{\text{PZ}} = 0.377$ ,  $Q_{\text{MZ}} = 0.542$  and  $Q_{\text{NZ}} = 0.081$ . The quantity of integrins for the whole cell was  $Q_{\text{PZ}} + Q_{\text{MZ}} + Q_{\text{NZ}} = 1$ .

Panel A represents the data for the integrin dynamics in the peripheral zone. The fit curve is exponential decay of second order (equation (12)). Panel B presents the

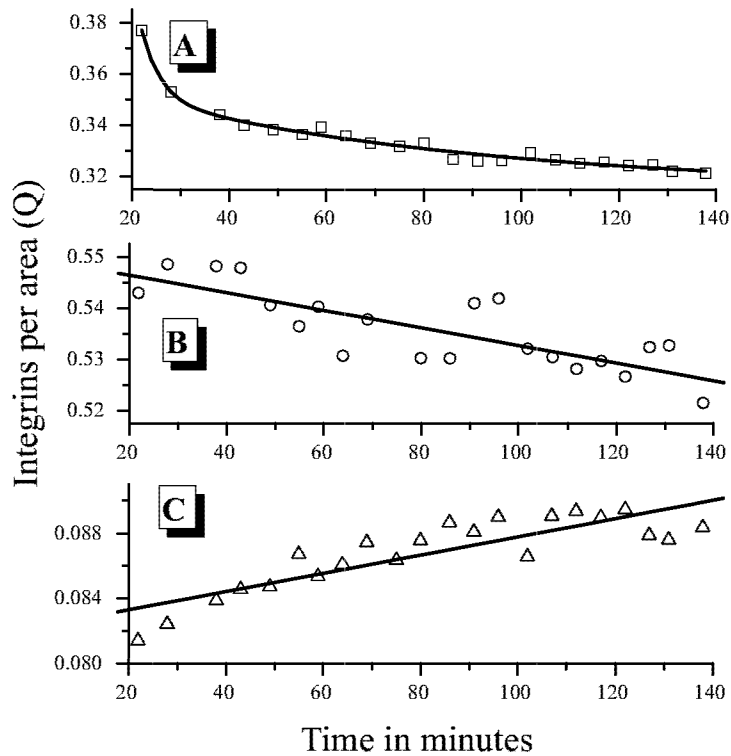


**Figure 4.** Changes in the quantity of integrins in the different zones of the cell during the time of experiment. The zones are shown in Fig. 1. Initial quantities of integrins were as follows: peripheral zone  $Q_{pz} = 0.377$ , middle zone  $Q_{mz} = 0.542$  and nuclear zone  $Q_{nz} = 0.081$ ;  $Q_{pz} + Q_{mz} + Q_{nz} = 1$ .

data for the middle zone. Fit to experimental points is a straight line with negative slope. In panel C are presented the changes in the central zone. Fit is also a straight line, but the slope is positive. All parameters of the fits are given in Section 3.

Each point represents the mean values of measurements and the standard errors of the means, which do not exceed 5%.

Figure 4 shows how the distributions of integrins in different zones change with the time. Integrins from PZ migrate centripetally to the MZ and the decrease in their quantity is presented in Panel A. Fitting a few models to the experimental points (open squares in Panel A) observed diminish coincides best to an exponential decay of second order

$$Q(t) = Q_{\min} + Q' \cdot \exp(-t/k_1) + Q'' \cdot \exp(-t/k_2) \quad (12)$$

where  $Q(t)$  is the specific quantity of integrins as a function of time  $t$  (in minutes). Experimentally obtained values for the constants were as follows:

The minimal quantity at time  $t \rightarrow \infty$  is  $Q_{\min} = 0.312 \pm 0.00076$ ,  $Q' = 0.066 \pm 0.0039$ ,  $Q'' = 0.021 \pm 0.002$ ,  $k_1 = 32 \pm 3$  and  $k_2 = 98.5 \pm 9.8$ .

Using the terminology of the classical kinetics, expression (12) represents a kinetic equation for three types of particles, first of them being the immobile integrins and their quantity is  $Q_{\min} = 0.312 \pm 0.00076$ . Having in mind the initial average quantity  $Q(t_0) = 0.377 \pm 0.004$ , the relative part of the immobile receptors is about  $82.76 \pm 0.66\%$  from all particles in PZ. The rest  $17.24 \pm 0.66\%$  are the mobile receptors, which migrate to MZ. A part of them are “fast” receptors with velocity constant  $1/k_1 = 0.031 \pm 0.0017$ . Finally, “slow” receptors have velocity constant  $1/k_2 = 0.01 \pm 0.0012$ . The ratio of  $Q'/Q'' = 3.143$  shows that “fast” receptors are about three times more than the “slow” ones, 12.75% and 4.25%, respectively.

For direct measuring of the integrin speeds were chosen the fastest moving particles and thus the fraction of “fast” receptors in PZ has average speed of  $0.353 \pm 0.02 \mu\text{m}/\text{min}$ ,  $n = 48$ ,  $p < 0.05$  (see Section 3.1). As the ratio of velocity constants of “fast” to “slow” receptors shows a value of 3.1, the speed of “slow” receptors can be easily calculated. It was  $0.114 \mu\text{m}/\text{min}$ .

Analysis of MZ (Panel B in Fig. 4) demonstrates a slow diminution of the integrin density in the range of 3.7%, which is statistically negligible, showing that the quantity of integrins in MZ remains approximately constant during the experiment and signifying that the penetration of integrins in MZ from the periphery is compensated by passing of other integrins to NZ.

Quantity of receptors in the central nuclear zone increases linearly in time with about 7.6%, manifesting a slight, but statistically significant accumulation of integrins around the cell nucleus.

#### 4. Discussion

The dynamics of integrin movements and organization is important for their proper interaction with ECM and tightly influences the function of these trans-membrane receptors. According to the latest knowledge, the rate of integrin movement is directly connected to the receptor mobility, the affinity to ligands, binding to ECM, induction of fibronectin fibrillogenesis [34], cell migration [4, 21], endocytosis and recycling of integrins [2, 5, 26, 27, 29] and other key cellular functions.

Here we found that the movement of integrins is not chaotic and is rather organized and directed from the periphery to the cell center. In fact other authors also report for such centripetal movement of integrins [14, 22, 25, 36], but they consider structures located mostly on the ventral cell surface and do not describe their

translocation in all cell membrane. Actually, this was the reason we wanted to create a new approach for measuring the integrin densities at different zones of the cell. The present study ascertains some chaotic movement of integrins, but it was in a comparatively small region around the cell center that we call NZ. Although, it was possible to apply methods for measuring the classical lateral diffusion of particles, known as FRAP, but we keep away from such study considering the generally oriented and active movement of integrins along the cytoskeleton. In our approach we used the direct tracing of individual clusters, as described in Section 2.

As far as the two types of integrin movement was registered, one directed from the periphery to the cell center (centripetal in PZ and MZ) and second, chaotic diffusion in NZ, we used the terms “velocity” (vector) and “speed” (scalar), respectively, having in mind their absolute values. The results had clearly shown that centripetal velocities in MZ are almost 50% higher than in the PZ (at a level of significance  $p < 0.05$ ,  $n = 44$ ), a fact that may be attributed to the absence of stable focal contacts in the MZ. Conversely, the lowered velocity of integrins in PZ may be explained by the higher concentration of tight bonds between the ECM and the cellular cytoskeleton existing in the focal adhesion complexes [1, 10, 23, 24]. Nevertheless, the speeds of integrin clusters in the central NZ, although chaotic, were significantly higher ( $p < 0.05$ ,  $n = 44$ ) than in PZ and lower ( $p < 0.05$ ,  $n = 44$ ) than in the MZ. This result may be explained with the hypothesis, that NZ is the place for endocytosis of these receptors. Indeed, many authors proposed that the centripetal movement is a part of endocytic pathway connected with the degradation and recycling of integrins into regions around the cell nucleus, where the Golgi apparatus is located [2, 5, 26, 27, 29]. In addition some authors suggested the presence of a locus for regulation of cell motility also located at the central region [4, 21].

Individual speeds of integrins give only limited information about the dynamical distribution of these receptors. Therefore, to make more detailed analysis we needed methods for quantification of the mass-related reorganization of these receptors. Crucial moment in this intention was the elimination of the distortion effect of the bleaching. Applied by us approach to create cell-specific correction functions is novel and permits sufficient normalization and analytical presentation of the data for integrin dynamics.

Another rationale in this work was the analysis of integrin densities at different cell zones, via applying the specially created mathematical model and algorithm. Exponential decay of integrin quantity in PZ demonstrates the “flash-like” reaction of the cell in respect to the integrin reorganization during fibroblast spreading on fibronectin. Moreover, in this zone we could identify three populations of integrins, immobilized, fast and slow. Immobilized are presumably the integrins located in focal contacts as their ratio was very close to the ratios of immobilized integrins

reported by Duband *et al* [8] and Palecek *et al* [21]. On the other hand, the calculated velocity (0.114  $\mu\text{m}/\text{min}$ ) of the slow receptors is in a good coincidence with these, measured by Smilenov *et al* [25] of 0.12  $\mu\text{m}/\text{min}$  for the moving focal adhesions. Their proportion in our experiments was 4.16% of all the integrin population. Conversely, the fast receptors (13.08%) that we propose are localized on the dorsal cell surface are not investigated up to now. The rate of their higher velocity of 0.353  $\mu\text{m}/\text{min}$  correlates with the speed of the actin retrograde flow measured by Vallotton *et al* [28] of 0.29  $\mu\text{m}/\text{min}$ . This fact is in a good agreement with the general concept for integrin functioning, according which the integrins works as a mechanical link that connect ECM with the cell cytoskeleton [10, 17, 31, 34]. On the other hand, tagging of integrins with antibodies mimics to a certain extent the physiological binding to ECM and thus stimulates the conformational changes, leading to the activation of the  $\beta_1$  integrin cytoplasmic tail. According to the latest knowledge, several intracellular anchor proteins, including talin,  $\alpha$ -actinin, and filamin mediate the direct linking of this subunit to the actin filaments [17]. This linking however, is presumably reversible as the integrins may further move along the actin filaments, which already explains the observed fast integrin movements on the dorsal cell surface.

The receptors in the middle zone represented highest mobility, but it was not oriented. This is presumably because they become closer to the hypothetic cell contractility center [4]. This view is in accordance with Palecek *et al* [21] who also suggest the presence of locus for regulation of cell motility located close to the central region. The quantity of integrins in the other cell regions remains practically constant, probably because the influx of receptors from PZ is equilibrated by passing of other integrins to NZ. This means however, that we have accumulation of integrins in the NZ. The biological significance of such relative concentration of integrins in the NZ is not clear. It is possible that here they enter the internalization pathway and “wait” for recycling. Further studies are obviously needed to answer the questions rised with this study.

## References

- [1] Adams J., *Cell-Matrix Contact Structures*, Cell Mol. Life Sci. **58** (2001) 371–392.
- [2] Altankov G. and Grinnell F., *Fibronectin Receptor Internalization and AP-2 Complex Reorganization in Potassium-Depleted Fibroblasts*, Exp. Cell Res. **216** (1995) 1–11.
- [3] Arroyo A., Garcya-Pardo A. and Sanchez-Madrid F., *A High Affinity Conformational State on VLA Integrin Heterodimers Induced by an Anti-B<sub>1</sub> Chain Monoclonal Antibody*, J. Biol. Chem. **268** (1993) 9863–9868.
- [4] Ballestrem C., Hinz Z., Imhof B. and Wehrle-Haller B., *Marching at the Front and Dragging Behind: Differential  $\alpha_v\beta_3$ -Integrin Turnover Regulates Focal Adhesion Behavior*, J. Cell Biol. **155** (2001) 1319–1332.

- [5] Bretscher M., *Endocytosis and Recycling of The Fibronectin Receptor in CHO Cells*, EMBO J. **8** (1989) 1341–1348.
- [6] Chen B. and Hemler M., *Multiple Forms of the Integrin VLA-2 Can be Derived From a Single  $\alpha 2$  cDNA Clone: Interconversion of Forms Induced by an Anti-B1 Antibody*, J. Cell Biol. **120** (1993) 537–543.
- [7] Cukierman E., Pankov R. and Yamada K., *Cell Interactions with Three-Dimensional Matrices*, Curr. Opin. Cell Biol. **14** (2002) 633–639.
- [8] Cruz M., Dalgard C. and Ignatius M., *Functional Partitioning of  $\beta_1$  Integrins Revealed by Activating and Inhibitory mAbs*, J. Cell Sci. **110** (1997) 2647–2659.
- [9] Duband J.-L., Nuckolls G., Ishihara A., Hasegawa T., Yamada K., Thiery J.-P. and Jacobson K., *Fibronectin Receptor Exhibits High Lateral Mobility in Embryonic Locomoting Cells but is Immobile in Focal Contacts and Fibrillar Streaks in Stationary Cells*, The Journal of Cell Biology **107** (1988) 1385–1396.
- [10] Geiger B., Bershadsky A., Pankov R. and Yamada K., *Transmembrane Extracellular Matrix – Cytoskeleton Crosstalk*, Nature Reviews (Molecular Cell Biology) **2** (2001) 793–805.
- [11] Humphrees M., McEvan P., Barton S., Buckley P., Bella J. and Mould A., *Integrin Structure: Heady Advances in Ligand Binding, but Activation Still Makes the Knees Wobble*, Trends in Biochemical Sciences **28** (2003) 313–320.
- [12] Hynes R., *Integrins: Versatility, Modulation and Signaling in Cell Adhesion*, Cell **69** (1992) 11–25.
- [13] Katz B.-Z., Zamir E., Bershadsky A., Kam Z., Yamada K. and Geiger B., *Physical State of the Extracellular Matrix Regulates the Structure and Molecular Composition of Cell-Matrix Adhesions*, Mol. Biol. Cell. **11** (2000) 1047–1060.
- [14] Kawakami K., Tatsumi H. and Sokabe M., *Dynamics of Integrin Clustering at Focal Contacts of Endothelial Cells Studied by Multimode Imaging Microscopy*, J. Cell. Sci. **114** (2001) 3125–3135.
- [15] Kovach N., Carlos T., Yee E. and Harlan J., *A Monoclonal Antibody to  $\beta_1$  Integrin (CD29) Stimulates VLA-Dependent Adherence of Leukocytes to Human Umbilical Vein Endothelial Cells and Matrix Components*, J. Cell Biol. **116** (1992) 499–509.
- [16] MBC1 *Integrins* (Fig. 19.65), In: Molecular Biology of the Cell, Fourth edition, Chapter V. Cells in Their Social Context, 19. Cell Junctions, Cell Adhesion, and the Extracellular Matrix, B. Alberts, A. Johnson, J. Lewis, M. Raff, K. Roberts and P. Walter Eds., Garland Science, Taylor and Francis Group, N.Y. (2002) <http://www.ncbi.nlm.nih.gov/books/bv.fcgi?rid=mboc4.figgrp.3597>
- [17] MBC2 *Cell Junctions* (Fig.19.12B). In: Molecular Biology of the Cell, Fourth edition, Chapter V. Cells in Their Social Context, 19. Cell Junctions, Cell Adhesion, and the Extracellular Matrix, B. Alberts, A. Johnson, J. Lewis, M. Raff, K. Roberts and P. Walter Eds., Garland Science, Taylor and Francis Group, N.Y. (2002) <http://www.ncbi.nlm.nih.gov/books/bv.fcgi?rid=mboc4.figgrp.3491>
- [18] Miyamoto S., Akiyama S. and Yamada K., *Synergistic Roles for Receptor Occupancy and Aggregation in Integrin Transmembrane Function*, Science **267** (1995) 883–885.

- 
- [19] Miyamoto S., Teramoto H., Coso O., Gutkind J., Burbelo P., Akiyama S. and Yamada K., *Integrin Function: Molecular Hierarchies of Cytoskeletal and Signaling Molecules*, J. Cell Biol. **131** (1995) 791–805.
- [20] Mould A., Garratt A., Askari J., Akiyama S. and Humphries M., *Identification of a Novel Anti-Integrin Mab that Recognizes a Ligand-Induced Binding Site Epitope on the  $\beta_1$  Subunit*, FEBS Lett. **363** (1995) 118–122.
- [21] Palecek S., Schmidt C., Lauffenburger D. and Horwitz A., *Integrin Dynamics on the Tail Region of Migrating Fibroblasts*, J. Cell Sci. **109** (1996) 941–952.
- [22] Pankov R., Cukierman E., Katz B.-Z., Matsumoto K., Lin D., Lin S., Hahn C. and Yamada K., *Integrin Dynamics And Matrix Assembly: Tensin-Dependent Translocation of A5 $\beta$ 1-Integrins Promotes Early Fibronectin Fibrillogenesis*, J. Cell Biol. **148** (2000) 1075–1090.
- [23] Petit V. and Thiery J.-P. *Focal Adhesions: Structure and Dynamics*, Biology of the Cell **94** (2000) 477–494.
- [24] Sastry S. and Burridge K., *Focal adhesions: A Nexus for Intracellular Signaling and Cytoskeletal Dynamics*, Exp. Cell. Res. **261** (2000) 25–36.
- [25] Smilenov L., Mikhailov A., Pelham Jr. R., Marcantonio E. and Gundersen G., *Focal Adhesion Motility Revealed in Stationary Fibroblasts*, Science **286** (1999) 1172–1174.
- [26] Sczekan M. and Juliano R., *Internalization of the Fibronectin Receptor is a Constitutive Process*, J. Cell. Physiol. **142** (1990) 574–580.
- [27] Tawil N., Wilson P. and Carbonetto S., *Integrins in Point Contacts Mediate Cell Spreading – Factors that Regulate Integrin Accumulation in Point Contacts vs. Focal Contacts*, J. Cell Biol. **120** (1993) 261–271.
- [28] Valloton P., Ponti A., Waterman-Storer C., Salmon E. and Danuser E., *Recovery, Visualization and Analysis of Actin and Tubulin Polymer Flow in Live Cells: A Fluorescence Speckle Microscopy Study*, Biophys. J. **85** (2003) 1289–1306.
- [29] Watts C. and Marsh D., *Endocytosis: What Goes in and How?*, J. Cell Sci. **103** (1992) 1–8.
- [30] Webb K., Hlady V. and Tresco P., *Relationships Among Cell Attachment, Spreading, Cytoskeletal Organization and Migration Rate for Anchorage-Dependent Cells on Model Surfaces*, J. Biomed. Mater. Res. **49** (2000) 362–368.
- [31] Wehrle-Haller B. and Imhof B., *The Inner Lives of Focal Adhesions*, Trends in Cell Biology **12** (2002) 382–389.
- [32] Wiseman P., Brown C., Webb D., Hebert B., Johnson N., Squier J., Ellisman M. and Horwitz A., *Spatial Mapping of Integrin Interactions and Dynamics During Cell Migration by Image Correlation Microscopy*, J. Cell Sci. **117** (2004) 5521–5534.
- [33] Yamada K. and Geiger B., *Molecular Interactions in Cell Adhesion Complexes*, Curr. Opin. Cell. Biol. **9** (1997) 76–85.
- [34] Yamada K., Pankov R. and Cukierman E., *Dimensions and Dynamics in Integrin Function*, Braz. J. Med. Biol. Res. **36** (2003) 959–966.

- [35] Zamir E. and Geiger B., *Molecular Complexity and Dynamics of Cell-Matrix Adhesions*, J. Cell Sci. **114** (2001) 3583–3590.
- [36] Zamir E., Katz M., Posen Y., Erez N., Yamada K., Katz B.-Z., Lin S., Lin D., Bershadsky A., Kam Z. and Geiger B., *Dynamics and Segregation of Cell-Matrix Adhesions in Cultured Fibroblasts*, Nature Cell Biol. **2** (2000) 191–196.
- [37] Zlatanov I., Lendlein A., Groth Th. and Altankov G., *Dynamics of  $\beta_1$ -integrins in Living Fibroblasts – Effect of Substratum Wettability*, Biophys. J. **89** (2005) 3555–3562.